

# Electromagnetic Modeling Of Beam Position And Phase Monitors For SNS Linac

Sergey S. Kurennoy

*Los Alamos National Laboratory, SNS-PO, MS H824, Los Alamos, NM 87545, USA*

**Abstract.** Electromagnetic modeling of the beam position monitors (BPMs) for the Spallation Neutron Source (SNS) linac has been performed with MAFIA. The signal amplitudes and phases on the BPM electrodes are computed as functions of the beam transverse position using time-domain 3-D simulations with an ultra-relativistic beam. An analytical model is then applied to extrapolate the results to lower beam velocities. It is shown that while the signal phases on the individual electrodes for an off-axis beam can differ from those for a centered beam by a few degrees, the phase of the summed signal from all electrodes is insensitive to the beam transverse position inside the device. Based on the analysis results, an optimal BPM design with 4 one-end-shortened 60-degree electrodes has been chosen. It provides a very good linearity and sufficient signal power for both position and phase measurements, while satisfying the linac geometrical constraints and mechanical requirements.

## INTRODUCTION

Beam position monitors (BPMs) in the SNS linac will deliver information about both the transverse position of the beam and the beam phase. Typical values for the position accuracy are on the order of 0.1 mm in the beam position within 1/3 of the bore radius  $r_b$  from the axis ( $r_b$  is between 1 cm and 2 cm for the normal conducting part of the linac). The beam phase accuracy is a fraction of the RF degree. The BPMs have a high signal processing frequency, equal to the microbunch repetition frequency in the linac,  $f_b=402.5$  MHz (or one of its lowest harmonics). A rather limited length along the beam line is available for BPM transducers, as usually in ion linacs, especially at low beam energies. This imposes certain restrictions on the linac BPM design. Using summed signals from the BPM electrodes for the linac beam-phase detection, e.g. see [1], requires some extra signal power, but has an obvious advantage that no additional devices on the beam line for phase measurements are required.

To study options for the transducers of the SNS linac BPMs, we use the EM code package MAFIA [2]. Electrostatic 2-D computations are used to adjust the BPM cross-section parameters to have 50- $\Omega$  transmission lines. Then 3-D static and time-domain computations are applied to calculate the electrode coupling. Time-domain 3-D simulations with an SNS beam microbunch passing through the BPM at a varying offset from the axis are used to compute the induced voltages on the electrodes as functions of time. After that an FFT procedure extracts the amplitudes and phases of the signal harmonics at individual outputs, as well as the amplitude and phase of the combined (summed) signal, versus the beam transverse position.

# BEAM POSITION AND PHASE MONITORS

## Electromagnetic Modeling

To conform the restrictions mentioned above, it was decided to choose 4-electrode BPM design with one-end-shortened stripline electrodes. A MAFIA models for the BPM consisting of a box with 4 electrodes on a beam pipe is shown in Fig. 1. The electrodes are flush with the beam pipe, shorted at one end, and have 50- $\Omega$  connectors on the other end. The beam pipe radius in the model is  $r_b=20$  mm, the electrode length along the beam is 40 mm, and their subtended angle is 60°. The 50- $\Omega$  terminations of the electrodes are modeled by filaments with discrete elements, 50- $\Omega$  resistors in this case.

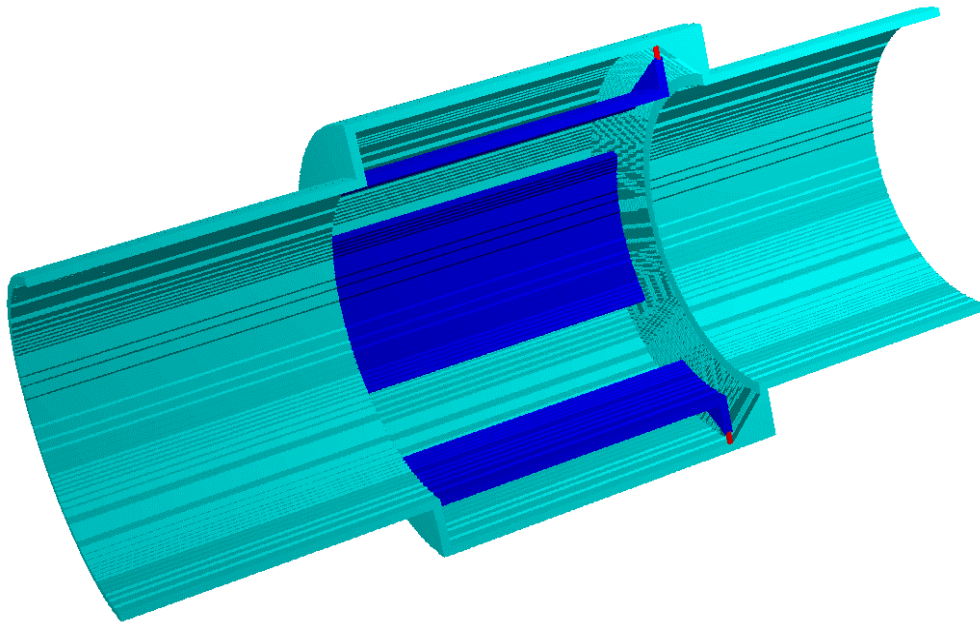


**FIGURE 1.** MAFIA model of SNS linac BPM (one-half cutout) with cone-tapered box and electrodes (dark-blue) with modified terminations (connectors are shown in red).

This design provides a rigid mechanical structure with a good repeatability from one device to another, so that detailed mappings will be required for a few BPMs only. The design is bi-directional, which may be useful in tight spots. It also saves four connectors, and since the remaining four are all on one end of the BPM, the device can be mounted close to quadrupoles. The disadvantage of the one-end-shortened electrodes is the difficulty of their proper matching with a 50- $\Omega$  connector on the other end, compared to the stripline electrodes having 50- $\Omega$  connectors on both ends. The signal power in a BPM transducer for a given beam current can be increased by increasing the length and width of the electrodes (lobes). Obviously, the electrode length is limited by available space on the beam line, in some cases as short as 2 inches. Wider electrodes generally provide a better linearity, but for very wide lobes the gap separating them is getting small, and one can expect a noticeable coupling. Within

these constraints, we considered and numerically modeled a few possible designs. The coupling between BPM electrodes was calculated in two different ways. In a static approximation we solve a 2-D electrostatic problem to find potentials on passive electrodes with a given potential on an active one. A similar procedure is used to adjust the BPM cross section for the electrodes to form 50- $\Omega$  transmission lines. In the dynamical 3-D problem, a 402.5-MHz *sin*-signal with the amplitude increasing to some level is fed into a connector of the active electrode, and the induced signals on the passive ones are calculated. In both cases, the coupling coefficients are defined as ratios of the potentials or voltage amplitudes:  $k_{12}=A_2/A_1$  for two adjacent electrodes, and  $k_{13}=A_3/A_1$  for two opposite ones. Figure 2 illustrates the static coupling between the BPM electrodes for three different BPM cross sections. Inserting the separators – the metal ridges connected to the BPM box and filling the gap between the adjacent electrodes – reduces the static coupling about two times. With the separators, the coupling of 60° electrodes (left) is reduced (center) to that of 45° electrodes (right).

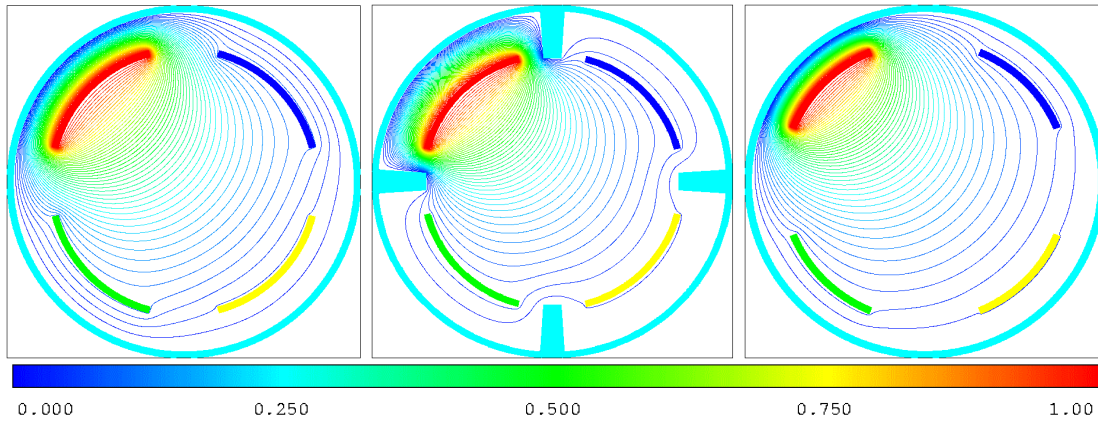


**FIGURE 2.** Electrostatic coupling in three BPMs: 60° electrodes (left), the same with separators (center), and 45° electrodes (right). The color of equipotential lines corresponds to the scale below.

Direct 3D time-domain computations with an ultra relativistic ( $\beta=1$ ) bunch passing the structure at the axis or parallel to the axis have been performed for a few layouts of the BPM transducers. A Gaussian longitudinal charge distribution of the bunch with the total charge  $Q=0.14$  nC and the rms length  $\sigma=5$  mm, corresponding to the 56-mA current in the baseline SNS regime with 2-MW beam power at 60 Hz, was used in the simulations. Unfortunately, the MAFIA time-domain code T3 at present cannot simulate the open (or waveguide) boundary conditions on the beam pipe ends for non-ultra relativistic ( $\beta<1$ ) beams. In the next section, the ultra relativistic MAFIA results are used to fix parameters of an analytical model of the BPM at  $\beta=1$ , and then to derive results for  $\beta<1$  analytically. For illustration, Fig. 3 shows the voltages on all four electrodes versus time for the case of a beam displaced from the chamber axis by  $x=r_b/2$  (half aperture) horizontally and by  $y=r_b/4$  vertically, and their corresponding Fourier transforms, for the BPM of Fig. 1. Indices  $R,T,L,B$  here refer to the right, top, left and bottom electrodes of the BPM. The Fourier spectra of the signals have first peaks near 2 GHz, that corresponds approximately to the wavelength  $\lambda/4=l$ .

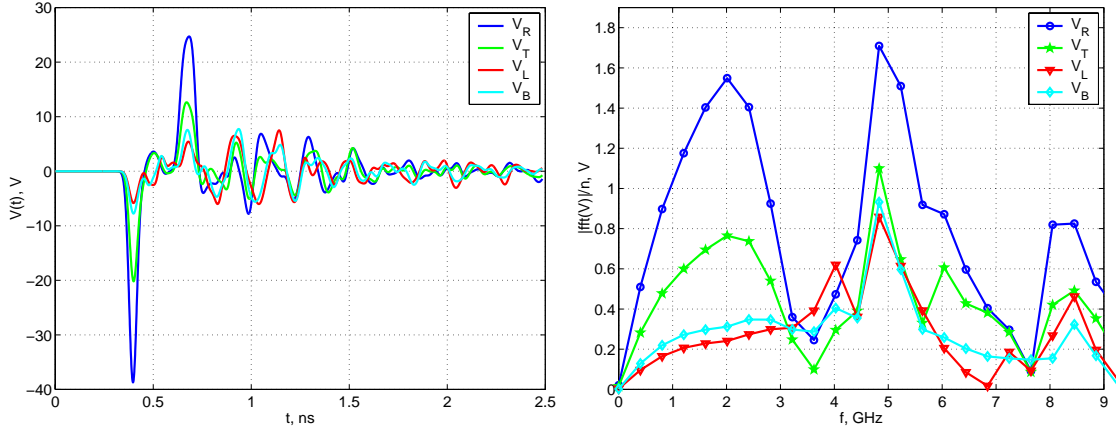


**FIGURE 3.** Signals on four BPM electrodes from a passing transversely displaced ( $x=r_b/2$ ,  $y=r_b/4$ ) bunch: left – voltages versus time during one period  $T=1/f_b=2.4845$  ns; right – normalized Fourier transform amplitudes (V) versus frequency.

Table 1 summarizes our simulation results for a few different BPM types. It lists the static and dynamic couplings, the maximal signal voltage on the electrodes from the on-axis beam, the amplitude and corresponding signal power of the 1<sup>st</sup> Fourier harmonic (at 402.5 MHz).

**TABLE 1. Comparison of Different Designs for 4-electrode SNS BPM (with on-axis beam).**

electrode shape	angle, °	length, mm	$k_{st12}$ ; $k_{st13}$ (%)	$k_{dyn12}$ ; $k_{dyn13}$ (%)	$ V(t) _{max}$ , V	$\tilde{A}_1$ , V	P, dBm
rectangular	45	26	0.13; 0.05	1.8; 0.55	13.5	0.118	-8.5
rectangular	60	26	0.21; 0.09	2.6; 0.74	14	0.155	-6.2
rect., w/separators	60	26	0.13; 0.05	1.1; 0.34	10	0.120	-8.4
2 50- $\Omega$ termin.	60	26	0.21; 0.09	1.4; 0.5	13	0.150	-6.5
rectangular	60	40	0.34; 0.15	3.6; 1.1	12.5	0.189	-4.5
tapered	60	40	same	3.6; 1.1	13.9	0.245	-2.2
tapered, cone box	60	40	same	3.7; 1.2	14	0.244	-2.3
taper, cone, separ.	60	40	0.13; 0.05	1.7; 0.57	11.5	0.161	-5.9
cone, mod. termin.	60	40	0.34; 0.15	5.1; 1.6	18	0.255	-1.9

One can see that the separators reduce the electrode coupling but at the same time the signal power decreases. Having two 50- $\Omega$  connectors on both ends of the electrode also reduces the dynamical coupling, with about the same signal power as in the one-end-shortened design. However, such a design is more complicated and more expensive, as well as less reliable mechanically, compared to the one-end-shortened version.

To study the BPM linearity, we perform simulations with the beam bunch passing through the BPM at different transverse positions. Some results for the BPM design with modified terminations (Fig. 1) are presented in Table 2. One can see that at high beam energies the signal power at 402.5 MHz changes between +4.6 dBm and -12.3

dBm as the beam position moves within a rather wide range,  $\{x,y \in (-r_b/2, r_b/2)\}$ . This corresponds to the signal dynamical range of 16.9 dB.

**TABLE 2. Amplitudes of Signal Harmonics on BPM Electrodes versus Beam Position.**

Position		@ 402.5 MHz					@ 805 MHz					
x/r	y/r	$\tilde{A}_R$	$\tilde{A}_T$	$\tilde{A}_L$	$\tilde{A}_B, V$	$\tilde{A}_\Sigma, V$	$\tilde{A}_R$	$\tilde{A}_T$	$\tilde{A}_L$	$\tilde{A}_B, V$	$\tilde{A}_\Sigma, V$	
0	0	0.255					1.021	0.44				
0.25	0	0.374	0.240	0.168	0.240	1.022	0.65	0.41	0.29	0.41	1.76	
0.25	0.125	0.368	0.291	0.166	0.196	1.021	0.64	0.50	0.28	0.34	1.76	
0.25	0.25	0.351	0.352	0.158	0.158	1.018	0.608	0.610	0.270	0.271	1.76	
0.5	0	0.540	0.194	0.103	0.194	1.031	0.95	0.33	0.18	0.33	1.78	
0.5	0.125	0.533	0.235	0.101	0.159	1.027	0.94	0.40	0.17	0.27	1.78	
0.5	0.25	0.510	0.282	0.096	0.129	1.016	0.90	0.48	0.16	0.22	1.75	
0.5	0.375	0.469	0.339	0.088	0.101	0.997	0.82	0.58	0.15	0.17	1.72	
0.5	0.5	0.408	0.409	0.077	0.077	0.970	0.702	0.704	0.135	0.135	1.67	

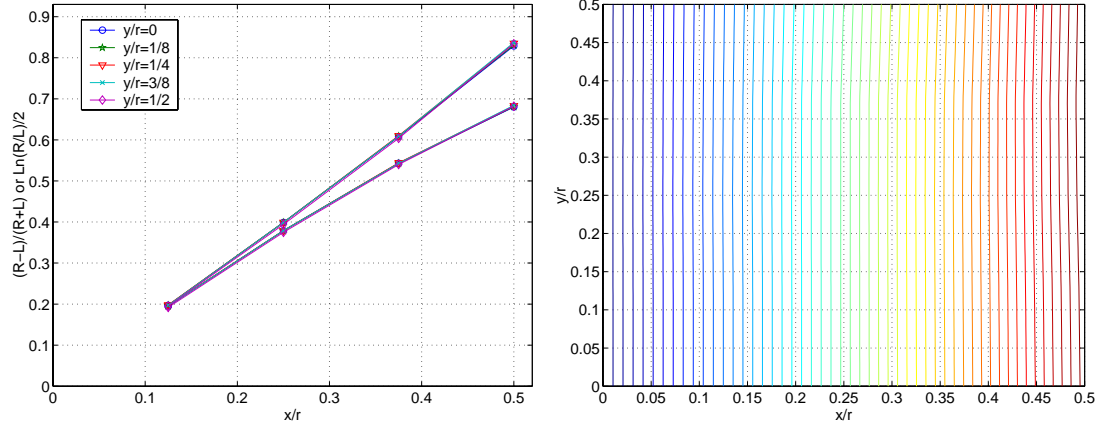


**FIGURE 4.** Horizontal ratio  $S$  of the signal harmonics at 402.5 MHz (top lines for  $S=\ln(\tilde{A}_R/\tilde{A}_L)/2$ , bottom ones for  $S=(\tilde{A}_R-\tilde{A}_L)/(\tilde{A}_R+\tilde{A}_L)$ ) versus the beam horizontal displacement  $x/r_b$ , for a few values of the beam vertical displacement  $y/r_b$  (left, see legend); contours of equal ratio  $S=\ln(\tilde{A}_R/\tilde{A}_L)/2$  (right).

The BPM linearity results are presented in Figs. 4. MAFIA data for the horizontal signal log ratio  $\ln(\tilde{A}_R/\tilde{A}_L)/2$  or the difference-over-sum  $(\tilde{A}_R-\tilde{A}_L)/(\tilde{A}_R+\tilde{A}_L)$  for different vertical beam positions overlap, so that it is difficult to distinguish between the five interpolating lines. Contours of equal log ratios projected onto  $x,y$ -plane in the right picture show rather small distortions visible only outside the region of about 1/3 of the aperture. One can conclude that the BPM design with  $60^\circ$  electrodes and the modified transitions (Fig. 1) is rather insensitive to the beam position in the direction orthogonal to the measured one, and has a good linearity. This BPM position sensitivity is  $20\log_{10}(\tilde{A}_R/\tilde{A}_L)/x \cong 1.4$  dB/mm. As for other designs considered, we have found that the linearity of BPMs with separators is much worse, in spite of the lower coupling.

## Analytical Model of BPM

Assuming an approximate axial symmetry of the beam pipe, the signals on the BPM electrodes with inner radius  $r_b$  and subtended angle  $\varphi$  can be calculated by integrating induced currents within the electrode angular extent. For a pencil beam

bunch passing the BPM at the transverse position  $x=r\cos\theta$ ,  $y=r\sin\theta$  at velocity  $v=\beta c$ , the signals are (e.g., [3])

$$E(f, r, \theta) = C \frac{\varphi}{2\pi} \left[ \frac{I_0(gr)}{I_0(gr_b)} + \frac{4}{\varphi} \sum_{m=1}^{\infty} \frac{I_m(gr)}{I_m(gr_b)} \sin(m(\phi/2 + \mu)) \cos(m(\theta - \nu)) \right] \quad (1)$$

where  $E=R, T, L, B$  are the Fourier components at frequency  $f$  of the signals on the corresponding electrodes, and the phases  $(\mu, \nu)$  are  $(0, 0)$  for  $R$ ,  $(0, \pi/2)$  for  $T$ ,  $(\pi, 0)$  for  $L$ ,  $(\pi, \pi/2)$  for  $B$ . Here  $I_m(z)$  are the modified Bessel functions, all dependence on frequency and energy enters through  $g=2\pi f/(\beta\gamma c)$ , and overall coefficient  $C$  depends on the bunch current and shape. The parameters of the BPM cross-section,  $r_b$  and  $\varphi$ , can be considered as “free” parameters of the model. Obviously, the induced current on an electrode in the real geometry is larger than an integral of the current density over the angle  $\varphi$  in an axisymmetric pipe of radius  $r_b$ , since more electric field lines from a passing bunch ends up on the electrode, compared to the circular pipe segment of the same radius and angular extent. We use Eqs. (1) to fit our MAFIA computation results for  $\beta=1$ , with some effective values of  $r_b$  and  $\varphi$ . One should expect these effective values to be larger than the geometrical ones.

One can introduce the coupling between the electrodes in the model to make it more realistic. If  $k_{12}$  denotes the coupling coefficient between adjacent electrodes, and  $k_{13}$  between the opposite ones, the coupled signals (1) can be written as

$$R_c = [R + k_{12}(T + B) + k_{13}L]/(1 + 2k_{12} + k_{13}) \quad (2)$$

and similar for  $T_c, L_c, B_c$ , via cyclic permutations of  $R, T, L, B$ .

We fit the MAFIA results at 402.5 MHz for the ratio  $S/(x/r_b)$ , where  $S$  is either the log ratio  $\ln(\tilde{A}_R/\tilde{A}_L)/2$  or the difference-over-sum ratio  $(\tilde{A}_R - \tilde{A}_L)/(\tilde{A}_R + \tilde{A}_L)$ , with our model. The best fit to the numerical data was obtained with the effective parameters  $r_{\text{eff}}=1.17r_b$ ,  $\varphi_{\text{eff}}=1.24\varphi$  ( $=74.5^\circ$ ), where  $r_b=20$  mm,  $\varphi=\pi/3$  rad are the geometrical values, and with  $k_{12}=k_{13}=0$ . It is interesting to note that the effective radius  $r_{\text{eff}}=23.4$  mm is close to the average of the electrode inner radius  $r_b=20$  mm and that of the BPM box, 26.5 mm, in agreement with earlier observations [4]. Attempts to introduce a non-zero coupling, even as small as 1%, lead to a rather wide spread between the curves for different  $y/r_b$ , so we have to conclude that the numerical results strongly suggest very small coupling between the BPM electrodes. This seems to contradict the dynamical coupling coefficients in Table 1. One should note, however, that Eq. (2) does not take into account that the inter-electrode coupling is mostly reactive, and  $k$ s in (2) should be complex, mostly imaginary (see more in the next section).

Matching the amplitude of 402.5-MHz harmonics from an on-axis ultra relativistic SNS beam bunch with Eqs. (1) fixes the constant  $C=1.232$ . The 402.5-MHz signal amplitudes for the displaced beams in Table 2 are then reproduced by the model with the accuracy of 1-2%. Assuming that these effective parameters of the model are applicable at lower beam velocities, we extrapolate  $\beta=1$  results to  $\beta<1$ . The signal power level for the on-axis beam is reduced by about 9 dB at  $\beta=0.073$  (2.5 MeV). For the strongest signal in the beam displacement range  $(-r_b/2, r_b/2)$  both vertically and horizontally, this reduction is 4.4 dB, and for the weakest one it is 12.9 dB. As a result, the dynamical range of the 402.5-MHz signal increases from about 17 dB for  $\beta=1$  to

about 25 dB at  $\beta=0.073$ , if the same radius of BPM is assumed. Of course, at the low-energy end the bore and BPM radii are smaller, which increases the power level.

### BPMs as phase probes

The application of the linac BPMs as the beam-phase probes and their favorable comparison with the capacitive probes has been studied earlier [1]. Here we present some results on the beam phase for the particular BPM design with  $60^\circ$  electrodes and the modified terminations (Fig. 1). For each beam displacement, the phases of the voltage Fourier transforms, as well as the amplitude and phase of the summed signal, have been calculated. Some results for the two harmonics are summarized in Table 3. Since we are mostly interested in the phase difference between the signals from an on-axis and off-axis beams, the beam phase of the centered beam ( $-170.09^\circ$  at 402.5 MHz and  $114.80^\circ$  at 805 MHz) is subtracted from the phases in the table. Our MAFIA computations used a relatively crude mesh with a step  $d=0.5$  mm in all three dimensions, that resulted in about 3 millions mesh points. One can roughly estimate the accuracy of calculated phases as corresponding to the time interval  $\Delta t=d/2/c=0.83$  ps, where  $c$  is the speed of light, corresponding to  $\pm 0.12^\circ$  for 402.5 MHz, and twice that at 805 MHz. The signal phases on individual electrodes differ by a few degrees, while the phases of the summed signals are equal, within this accuracy interval, for all beam displacements. The only exception is possibly the case of a rather strong offset  $x=r_b/2, y=r_b/2$  at 805 MHz. However, even in this case the deviation is only about  $0.6^\circ$ , which could be just as well a numerical effect, and it is very small compared to the phase difference for the individual electrodes that spans about  $17^\circ$  in this case.

**TABLE 3. Phases of Signal Harmonics on BPM Electrodes versus Beam Position.**

Position		@ 402.5 MHz					@ 805 MHz				
x/r	y/r	$\phi_R$	$\phi_L$	$\phi_T$	$\phi_B, ^\circ$	$\phi_\Sigma, ^\circ$	$\phi_R$	$\phi_L$	$\phi_T$	$\phi_B, ^\circ$	$\phi_\Sigma, ^\circ$
0	0			0		0			0		0
0.25	0	0.94	-0.39	-1.25	-0.39	-0.04	1.90	-0.62	-3.01	-0.62	-0.08
0.25	0.125	0.89	0.14	-1.34	-0.98	-0.04	1.86	0.61	-3.22	-2.09	-0.06
0.25	0.25	0.71	0.64	-1.66	-1.63	-0.04	1.73	1.61	-3.90	-3.85	-0.04
0.5	0	1.68	-1.67	-2.85	-1.67	-0.03	2.96	-2.73	-7.57	-2.73	-0.18
0.5	0.125	1.65	-1.00	-2.97	-2.39	-0.03	2.99	-0.86	-7.85	-4.99	-0.13
0.5	0.25	1.57	-0.35	-3.35	-3.18	-0.03	3.06	0.76	-8.77	-7.52	0.01
0.5	0.375	1.39	0.30	-4.06	-4.09	-0.02	3.19	2.13	-10.55	-10.37	0.26
0.5	0.5	1.02	0.95	-5.23	-5.18	0.00	3.36	3.23	-13.72	-13.60	0.59

The behavior of the signal phases versus the beam vertical position is shown in Figs. 5 for two particular horizontal deflections of the beam. As one can see, the signal phases on both horizontal electrodes behave similarly, but the phase changes on the vertical electrodes have opposite signs as the beam vertical position changes. At the same time, the phase of the summed signal remains equal to that of the on-axis beam, well within the computational errors (the error bars are shown only for the summed signal). We have modeled numerically only the  $\beta=1$  case, so the beam fields reach the individual electrodes simultaneously independent of the beam transverse position: in Fig. 3, the two peaks of  $V(t)$  – from the bunch passing the gap and then its reflection at the short, – are aligned for all electrodes. However, the stronger signals from the

electrodes that are closer to the beam, produce, via the reactive electrode coupling, some large voltage peaks at the furthest from the beam electrodes at later moments, see in Fig. 3, and this introduces the signal phase differences. A simple equivalent-circuit model explaining this effect was suggested in [5].

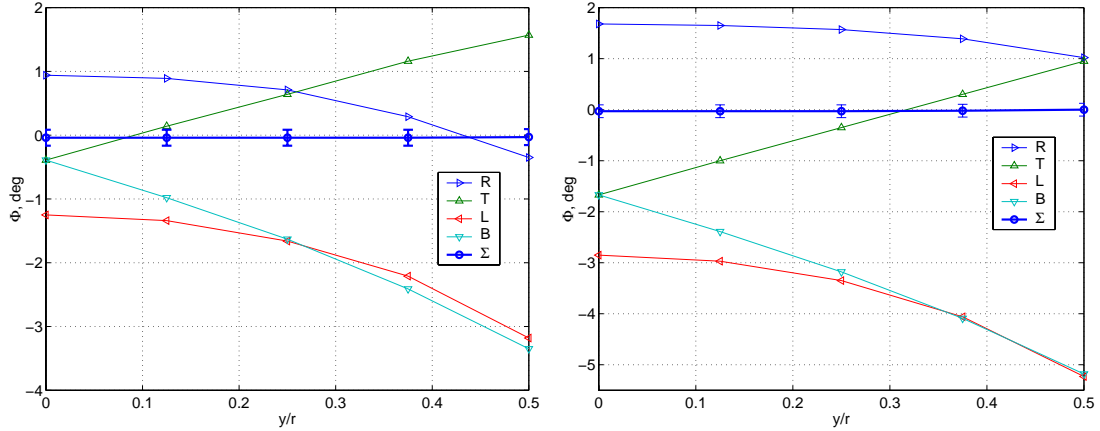


**FIGURE 5.** 402.5-MHz signal phases on four BPM electrodes and for the summed signal versus beam vertical displacement  $y/r_b$ , for the beam horizontal displacement  $x/r_b=1/4$  (left) and  $x/r_b=1/2$  (right).

## SUMMARY

Electromagnetic MAFIA modeling of the SNS linac BPMs has been performed. The signal amplitudes and phases on the BPM electrodes are computed as functions of the beam transverse position. The phases on the individual electrodes for an off-axis beam can differ from those for a centered beam by a few degrees, but the phase of the combined signal is insensitive to the beam transverse position. Based on the analysis results, an optimal BPM design with 4 one-end-shortened 60-degree electrodes has been chosen. It provides a good linearity and sufficient signal power for both position and phase measurements, while satisfying the geometrical and mechanical requirements.

The author would like to acknowledge useful discussions with A.V. Aleksandrov, J.F. O’Hara, J.F. Power, and R.E. Shafer.

## REFERENCES

1. Kurennoy, S.S., “On Beam Phase Detectors for SNS Linac”, Tech memo SNS: 99-65, Los Alamos, 1999; “Beam Position Monitors for SNS Linac”, Tech memo SNS: 2000-011, Los Alamos, 2000.
2. MAFIA Release 4.20, CST GmbH, Darmstadt, 1999.
3. Shafer, R.E., “Beam Position Monitor Sensitivity for Low- $\beta$  Beams” in *Beam Instrumentation Workshop, Santa Fe, NM, 1993*, edited by R.E. Shafer, AIP Conference Proceedings 319, New York: American Institute of Physics, 1994, pp. 303-308.
4. Shafer, R.E., “Beam Position Monitoring” in *Accelerator Instrumentation, Upton, NY, 1989*, edited by E.R. Beadle and V.J. Castillo, AIP Conference Proceedings 212, New York: American Institute of Physics, 1990, pp. 26-58.
5. Aleksandrov, A.V., “Influence of Inter-Electrode Coupling on BPM Performance”, SNS ORNL AP Group Tech Note 14, Oak Ridge, 2000.